Co-published by
Institute of Fluid-Flow Machinery
Polish Academy of Sciences
Committee on Thermodynamics and Combustion
Polish Academy of Sciences

http://www.imp.gda.pl/archives-of-thermodynamics/

Thermal and entropic behaviour of unsteady nanofluid flow in a permeable-walled Couette system

Michael Hamza Mkwizu[a*], Oluwole Daniel Makinde[b]

[a]Sokoine University of Agriculture, Departmentof Mathematics and Statistics, Chuo Kikuu, P.O. Box 3000, Morogoro, Tanzania
[b] Stellenbosch University, Facultyof Military Science, Private Bag X2, Saldanha 7395, South Africa
*Corresponding author email: mkwizu@sua.ac.tz

Received: 13.03.2025; revised: 25.10.2025; accepted: 29.10.2025

Abstract

This study examines the energy dissipation mechanisms in unsteady nanofluid flow confined between two permeable walls under a generalised Couette flow configuration, with a particular emphasis on entropy generation and convective heat transfer effects. Such an analysis is of growing significance in advanced thermal management applications, including industrial cooling processes, microelectronic systems, renewable energy technologies and biomedical devices, where nanofluids are increasingly employed to enhance thermal performance. The governing partial differential equations, derived from the conservation principles of mass, momentum, and energy, are solved numerically using a semi-discretisation finite-difference approach in conjunction with a Runge-Kutta-Fehlberg integration algorithm. Comprehensive results for velocity distribution, temperature field, skin friction coefficient, Nusselt number, entropy generation rate and Bejan number are presented and discussed. The findings reveal, among other trends, that increasing injection/suction rates and the Biot number reduce the Nusselt number, entropy generation rate and Bejan number at the stationary lower wall, while simultaneously enhancing these quantities at the upper moving wall. These results highlight the dual role of boundary conditions and thermal parameters in governing irreversibility, heat transfer efficiency and overall system performance. By offering insights into the minimisation of entropy-related losses, this work contributes to the design of more energy-efficient and sustainable nanofluid-based thermal systems.

Keywords: Transient Couette flow; Nanofluid; Suction/Injection; Irreversibility analysis; Numerical simulation

Vol. 46(2025), No. 4, 165–176; doi: 10.24425/ather.2025.156847

Cite this manuscript as: Mkwizu, M.H., & Makinde, O.D. (2025). Thermal and entropic behaviour of unsteady nanofluid flow in a permeable-walled Couette system. *Archives of Thermodynamics*, 46(4), 165–176.

1. Introduction

The study of thermodynamic analysis of unsteady Couette flow of nanofluids in a porous wall channel with convective cooling is significant due to its implications in heat transfer enhancement, energy efficiency and fluid dynamics in advanced engineering applications [1]. Nanofluids, which are suspensions of nanoparticles in a base fluid, exhibit superior thermal properties compared to conventional fluids, making them highly valuable in optimising heat dissipation in various systems [2].

Moreover, the properties of nanofluids can also be tailored for specific applications by adjusting the type, size and concentration of nanoparticles in the suspension. This allows for customisation of the thermal properties of nanofluids to meet the requirements of different heat transfer systems. Choi [3] introduced the concept of nanofluids, highlighting their superior thermal conductivities compared to traditional fluids. Analysis of unsteady heat and mass transfer in rotating magnetohydrodynamic (MHD) convection flow over a porous vertical plate has been conducted by Narmathaa and Kavitha. The results show

Nomenclature

a – channel width, m
Be – Bejan number
Bi – Biot number
$(c_p)_f$ – specific heat of the base fluid, J/(kg K)
$(c_p)_s$ – specific heat of nanoparticles, J/(kg K)
C_f – skin friction coefficient
Ec – Eckert number
k_f – thermal conductivity of the base fluid, W/(m K)
k_{nf} – nanofluid thermal conductivity, W/(m K)
k_s – thermal conductivity of nanoparticles, W/(m K)
N_{FFI} – fluid friction irreversibility
N_{HTI} – heat transfer irreversibility
Ns – dimensionless entropy generation rate
Nu – Nusselt number
P – nanofluid pressure, Pa
Pr – Prandtl number
Re – Reynolds number
S_G – entropy generation rate, W/(m^3 K)
t – time, s
T – temperature of the nanofluid, K
T_w – lower stationary wall temperature, K
u – nanofluid velocity in the x-direction, m/s

Greek symbols

α_{nf} – thermal diffusivity of the nanofluid, m^2/s
μ_{nf} – dynamic viscosity of the nanofluid, kg/(s m)
ρ_{nf} – density of the nanofluid, kg/m^3
ρ_f – density of the base fluid, kg/m^3
ρ_s – density of the nanoparticle, kg/m^3
φ – nanoparticles volume fraction

Subscripts and Superscripts

f – base fluid
nf – nanofluid
s – nanoparticle

Abbreviations and Acronyms

PDE – partial differential equation
MOL – method of lines

that the velocity and temperature decrease as the Prandtl number increases [4]. Unsteady Couette flow, characterised by fluid motion induced by shear between two parallel plates, plays a vital role in industrial processes, such as lubrication, polymer manufacturing and microfluidics, where real-time variations in flow can significantly influence system efficiency [5]. In studies involving nanofluid dynamics within confined geometries like channels, the Couette flow configuration is frequently employed, typically involving one moving surface and one stationary. This model serves as a fundamental framework for analysing shear-driven flows in nanofluid systems, offering valuable insights into how nanoparticle size and concentration affect flow behaviour and heat transfer. Notably, researchers such as Abu-Nada and Chamkha [6] and Ali et al. [7] have demonstrated that incorporating nanoparticles not only modifies flow dynamics but also enhances thermal conductivity and overall flow performance.

The incorporation of porous walls introduces permeability effects that significantly influence thermal regulation, pressure distribution and cooling efficiency, particularly in heat exchangers, biomedical devices and energy systems [8]. The introduction of permeable walls in nanofluid systems adds a layer of complexity to the analysis, as fluid can infiltrate or be sucked through the porous surfaces, which impacts both the flow rate and heat transfer efficiency. The concept of wall permeability has been explored by Kasaeian et al. [9], who investigated nanofluid flow in porous media and found that permeability significantly affects the flow and thermal characteristics. When coupled with convective cooling, the permeable walls can act as heat sinks, enhancing the overall heat transfer by facilitating the continuous replacement of hot fluid with cooler fluid from the surroundings. Convective cooling, as highlighted by Kakac and Pramuanjaroenkij [10], plays a crucial role in such systems by promoting efficient heat dissipation. The cooling effect is further augmented in systems involving nanofluids due to the higher thermal conductivity of these fluids. Studies by Shanthi et al. [11] and Malik et al. [12] have shown that the use of porous materials for convective cooling significantly boosts the heat dissipation rate, especially when coupled with nanofluids, making these systems highly efficient in industrial applications, such as electronic cooling. Convective cooling mechanisms play a pivotal role in thermal management technologies, such as microprocessors, fuel cells and aerospace heat shielding, ensuring optimal operating temperatures and reduced entropy generation [13].

The thermodynamic analysis of unsteady nanofluid Couette flow, particularly in a permeable wall channel, presents several challenges, especially in terms of understanding the time-dependent effects on heat transfer and energy dissipation. The unsteady flow introduces transient behaviours, which require careful modelling to account for variations in temperature and velocity profiles over time. Ndelwa et al. [14] emphasised the importance of entropy generation analysis in evaluating the thermodynamic efficiency of such systems, as it offers insights into the irreversibilities caused by viscosity, heat transfer and unsteady flow dynamics. The study of entropy generation in unsteady nanofluid systems provides a comprehensive view of the energy losses and potential for optimisation. Oztop and Abu-Nada [15] further explored how the unsteady flow conditions in a permeable channel increase entropy generation due to the time-varying nature of temperature and velocity fields. This, coupled with the effects of convective cooling, which continuously replenishes the hot fluid with cooler nanofluid, helps mitigate some of the thermodynamic inefficiencies, making the system more effective in energy dissipation and heat transfer enhancement [16,17]. Ali et al. [18] conducted a numerical investigation of the transient flow behaviour of silica nanofluids over a stretching cylinder, considering the influence of various nanoparticle shapes and Joule heating. Gorai et al. [20] carried out a theoretical study on how nanofluids affect the thermodynamic performance of flat-plate solar collectors. As the thermodynamic understanding of these systems continues to evolve, future research should focus on improving the models that de-

scribe the transient behaviours and optimising the configurations for maximum thermodynamic efficiency in nanofluid cooling applications.

This study analyses entropy generation in unsteady Couette flow of Cu-water nanofluid with convective cooling through permeable walls, providing a measure of irreversibility and energy loss. These insights support the development of more efficient thermal management and lubrication systems. The research has broad applications, including solar collectors, nuclear reactors, drug delivery systems, artificial organs, turbine cooling, aerodynamic heating control and advanced microfluidic devices. By combining nanofluid thermodynamics, porous media flow and convective cooling principles, the study offers valuable guidance for next-generation cooling technologies, sustainable energy systems and optimised industrial processes. According to the literature, this problem has not been exhaustively investigated; our objective is to fill this gap. The originality and novelty of the present study are outlined as follows:

- It provides a unique investigation of the unsteady thermal and entropic behaviour of nanofluid flow in a Couette system, emphasizing time-dependent effects and the role of nanoparticle-enhanced heat transfer, which are often neglected in existing models;
- It explores the impact of wall permeability, through suction and injection, on the boundary-layer development and entropy generation, offering fresh insights into thermodynamic irreversibility and flow regulation in advanced thermal systems.
- It establishes a comprehensive theoretical and numerical framework by employing the method of lines and adaptive Runge-Kutta-Fehlberg integration to analyse transient velocity, temperature and entropy characteristics in nanofluid-based configurations relevant to microfluidics, energy systems and heat transfer optimisation.

In the following sections, the model is formulated, analysed and numerically tackled. Pertinent results are presented graphically and discussed.

2. Mathematical model

Consider the unsteady laminar Couette flow of a viscous, incompressible water-based nanofluid containing copper nanoparticles through a parallel plate channel with permeable walls. The fluid is uniformly injected into the channel through the lower wall, while a uniform suction occurs at the moving upper plate, as illustrated in Fig. 1.

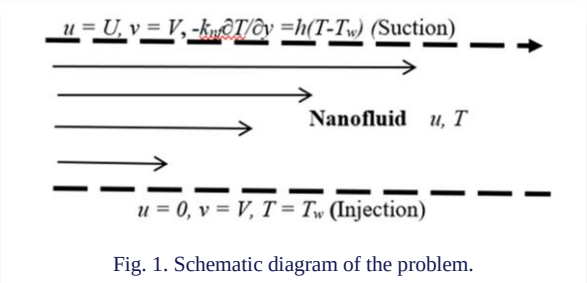

Fig. 1. Schematic diagram of the problem.

Based on the above assumptions, the governing equations for the momentum and energy of the nanofluid in one dimension can be expressed as follows.

$$\frac{\partial u}{\partial \bar{t}} + V\frac{\partial u}{\partial y} = -\frac{1}{\rho_{nf}}\frac{\partial P}{\partial x} + \frac{\mu_{nf}}{\rho_{nf}}\frac{\partial^2 u}{\partial y^2}, \tag{1}$$

$$\frac{\partial T}{\partial \bar{t}} + V\frac{\partial T}{\partial y} = \alpha_{nf}\frac{\partial^2 T}{\partial y^2} + \frac{\alpha_{nf}\mu_{nf}}{k_{nf}}\left(\frac{\partial u}{\partial y}\right)^2, \tag{2}$$

$$S_G = \underbrace{\frac{k_{nf}}{T_w^2}\left(\frac{\partial T}{\partial y}\right)^2}_{N_{HTI}} + \underbrace{\frac{\mu_{nf}}{T_w}\left(\frac{\partial u}{\partial y}\right)^2}_{N_{FFI}}, \tag{3}$$

where S_G is the entropy generation rate, N_{HTI} is the heat transfer irreversibility and N_{FFI} is the fluid friction irreversibility. The appropriate initial and boundary conditions are:

$$u(y,0) = 0,\ T(y,0) = T_w, \tag{4}$$

$$u(0,\bar{t}) = 0,\ T(0,\bar{t}) = T_w, \tag{5}$$

$$u(a,\bar{t}) = U,\ k_{nf}\frac{\partial T}{\partial y}(a,\bar{t}) = h[T(a,\bar{t}) - T_w], \tag{6}$$

where u is the nanofluid velocity in the x-direction, T is the temperature of the nanofluid, P is the nanofluid pressure, $\bar{t}$ is the time, a is the channel width, T_w is the lower stationary wall temperature, μ_{nf} is the dynamic viscosity of the nanofluid, k_{nf} is the nanofluid thermal conductivity, ρ_{nf} is the density of the nanofluid and α_{nf} is the thermal diffusivity of the nanofluid. The properties of the nanofluid are given by the formulas [6,10,13,17,19,20]:

$$\mu_{nf} = \frac{\mu_f}{(1-\varphi)^{2.5}},\ \rho_{nf} = (1-\varphi)\rho_f + \varphi\rho_s,$$

$$\frac{k_{nf}}{k_f} = \frac{(k_s+2k_f)-2\varphi(k_f-k_s)}{(k_s+2k_f)+\varphi(k_f-k_s)}, \tag{7}$$

$$\alpha_{nf} = \frac{k_{nf}}{(\rho c_p)_{nf}},\quad (\rho c_p)_{nf} = (1-\varphi)(\rho c_p)_f + \varphi(\rho c_p)_s,$$

where φ represents the nanoparticle volume fraction, ρ_f represents the density of the base fluid and ρ_s is the density of the nanoparticle, k_f is the thermal conductivity of the base fluid, and k_s is the thermal conductivity of the nanoparticles. The heat capacities of the base fluid and nanoparticles are represented by $(\rho c_p)_f$ and $(\rho c_p)_s$, respectively. Table 1 presents the thermophysical properties of water and copper nanoparticles.

Table 1. Thermophysical properties of nanofluid [6,10,13,17,19,20].

Physical properties	Fluid phase (water)	Copper (Cu)
C_p (J/kg K)	4179	385
ρ(kg/m^3)	997.1	8933
k(W/m K)	0.613	401

The following dimensionless variables and parameters are introduced, as follows:

$$\theta = \frac{T-T_w}{T_w},\ W = \frac{u}{U},\ t = \frac{\bar{t}V}{a},\ \upsilon_f = \frac{\mu_f}{\rho_f},\ \bar{P} = \frac{Pa}{\mu_f U},\ A = -\frac{\partial \bar{P}}{\partial X},$$

$$X = \frac{x}{a},\ \eta = \frac{y}{a},\ Ns = \frac{S_G a^2}{k_f},\ \mathrm{Pr} = \frac{\mu_f c_{pf}}{k_f},\ \mathrm{Ec} = \frac{U^2}{c_{pf}T_w}, \quad (8)$$

$$\tau = \frac{(\rho c_p)_s}{(\rho c_p)_f},\ m = \frac{(k_s+2k_f)+\varphi(k_f-k_s)}{(k_s+2k_f)-2\varphi(k_f-k_s)},\ \mathrm{Re} = \frac{Va}{\upsilon_f},\ \mathrm{Bi} = \frac{ha}{k_f}.$$

The governing equations (Eqs. (1)-(3)) in the dimensionless form can be written as:

$$\frac{\partial W}{\partial t} = \frac{A}{\mathrm{Re}\left[(1-\varphi)+\varphi\frac{\rho_s}{\rho_f}\right]} + \frac{1}{\mathrm{Re}\left[(1-\varphi)+\varphi\frac{\rho_s}{\rho_f}\right](1-\varphi)^{2.5}}\frac{\partial^2 W}{\partial \eta^2} - \frac{\partial W}{\partial \eta}, \quad (9)$$

$$\frac{\partial \theta}{\partial t} = \frac{1}{\mathrm{RePr}\, m(1-\varphi+\varphi\tau)}\frac{\partial^2 \theta}{\partial \eta^2} + \frac{\mathrm{Ec}}{\mathrm{Re}(1-\varphi)^{2.5}(1-\varphi+\varphi\tau)}\left(\frac{\partial W}{\partial \eta}\right)^2 - \frac{\partial \theta}{\partial \eta}, \quad (10)$$

$$Ns = \frac{k_{nf}}{k_f}\left(\frac{\partial \theta}{\partial \eta}\right)^2 + \mathrm{EcPr}\frac{\mu_{nf}}{\mu_f}\left(\frac{\partial W}{\partial \eta}\right)^2, \quad (11)$$

with the initial and boundary conditions given as

$$\left.\begin{array}{c} \theta(0,t) = 0, \quad \theta(\eta,0) = 0, \\ W(\eta,0) = 0, \\ W(0,t) = 0, \\ W(1,t) = 1, \\ \frac{\partial \theta}{\partial \eta}(1,t) = -m\mathrm{Bi}\theta(1,t). \end{array}\right\}. \quad (12)$$

Other quantities of practical interest in this study are the skin friction coefficient (C_f), the local Nusselt number (Nu), and the Bejan number (Be), which are defined as:

$$C_f = \frac{\mu_{nf}}{\mu_f}\frac{\partial W}{\partial \eta}\Big|_{\eta=0,1},\ \mathrm{Nu} = -\frac{k_{nf}}{k_f}\frac{\partial \theta}{\partial \eta}\Big|_{\eta=0.1},\ \mathrm{Be} = \frac{1}{1+Q}, \quad (13)$$

where $Q = \frac{N_{FFI}}{N_{HTI}}$ is the irreversibility ratio and

$$N_{HTI} = \frac{k_{nf}}{k_f}\left(\frac{\partial \theta}{\partial \eta}\right)^2, \quad N_{FFI} = \mathrm{EcPr}\frac{\mu_{nf}}{\mu_f}\left(\frac{\partial W}{\partial \eta}\right)^2. \quad (14)$$

3. Numerical procedures

Equations (9)–(12) form a system of nonlinear initial boundary value problems (IBVPs) that are solved numerically using a semi-discretisation finite-difference method known as the method of lines (MOL) [19] (see Fig. 2). We divide the spatial interval $0 \le \eta \le 1$ into Nequal parts, where the grid size $\Delta\eta = 1/N$ and grid points are defined as $\eta_i = (i-1)\Delta\eta$ for $1 \le i \le N+1$. This discretisation utilises a linear Cartesian mesh and a uniform grid to calculate finite differences. The first and second spatial derivatives in Eqs. (9)–(10) are approximated using second-order central finite differences.

Let $W_i(t)$ and $\theta_i(t)$ represent approximations of $W(\eta_i, t)$ and $\theta(\eta_i, t)$, respectively. The semi-discrete system for the problem then becomes:

$$\frac{dW}{dt} = \frac{A}{\mathrm{Re}\left[(1-\varphi)+\varphi\frac{\rho_s}{\rho_f}\right]} +$$

$$+ \frac{1}{\mathrm{Re}\left[(1-\varphi)+\varphi\frac{\rho_s}{\rho_f}\right](1-\varphi)^{2.5}}\left(\frac{W_{i+1}-2Wi+W_{i-1}}{(\Delta\eta)^2}\right) - \left(\frac{W_{i+1}-W_{i-1}}{2\Delta\eta}\right), \quad (15)$$

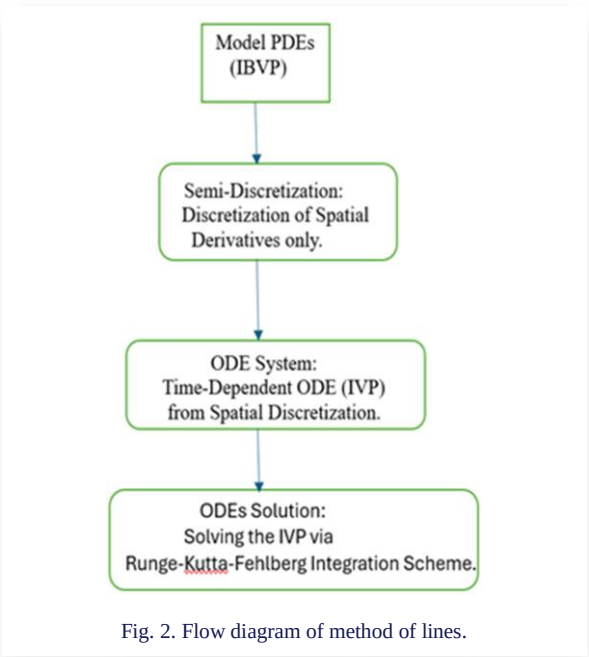

Fig. 2. Flow diagram of method of lines.

$$\frac{d\theta}{dt} = \frac{1}{\mathrm{RePr}\, m(1-\varphi+\varphi\tau)}\left[\frac{\theta_{i+1}-2\theta_i+\theta_{i-1}}{(\Delta\eta)^2}\right] +$$

$$+ \frac{Ec}{\mathrm{Re}(1-\varphi)^{2.5}(1-\varphi+\varphi\tau)}\left(\frac{W_{i+1}-W_{i-1}}{2\Delta\eta}\right)^2 - \left(\frac{\theta_{i+1}-\theta_{i-1}}{2\Delta\eta}\right). \quad (16)$$

Equations (15) and (16) represent a system of first-order ordinary differential equations with known initial conditions. The convergence of the MOL used to solve this initial boundary value problem with the Runge-Kutta-Fehlberg (RKF) method is assured, as it depends on the combined effects of accurate spatial discretisation and adaptive time-stepping control inherent in the RKF scheme.

In this approach, the spatial derivatives in the governing partial differential equations (PDEs) are discretised using a second-order central difference scheme, which converts the PDEs into a system of ordinary differential equations (ODEs) in time. The RKF method, an explicit Runge-Kutta algorithm of orders four and five, advances the solution in time by automatically adjusting the step size according to the estimated local truncation error between the two embedded approximations. Convergence is achieved when the spatial discretisation reliably captures the behaviour of the spatial derivatives as the mesh is refined and the time integration remains stable under the RKF's adaptive error control mechanism.

Since the method satisfies both consistency and stability conditions, the Lax equivalence theorem guarantees convergence of the overall numerical solution. Moreover, the resulting initial value problem can be solved iteratively using the Runge-Kutta-Fehlberg method, implemented using Maple software. To validate the accuracy of the numerical procedure and establish a benchmark for the present analysis, a special case of the current model is compared with previously published results for the velocity profile reported in [21]. This validation is performed under a steady-state condition for a conventional fluid ($\varphi = 0$)

Table 2. Velocity profile – comparison with the results from [21] for steady state when $\varphi = 0$, $A = 1$ and Re = 1.

η	Ref. [21] w(η)	Present $w(\eta)$
0	0	0
0.1	0.038792	0.0387930
0.2	0.071148	0.0711488
0.3	0.096390	0.0963903
0.4	0.113769	0.1137695
0.5	0.122459	0.1224593
0.6	0.121546	0.1215460
0.7	0.110019	0.1100195
0.8	0.086763	0.0867637
0.9	0.050544	0.0505450
1.0	0	0

confined between stationary permeable walls, as presented in Table 2. The comparison demonstrates excellent agreement in both qualitative trends and quantitative values, thereby confirming the reliability of the adopted computational approach.

4. Results and discussion

This section explores the influence of emerging parameters on Cu-water nanofluid flow and its heat transfer characteristics. The results from computational analyses are comprehensively presented in Figs. 3–26. The selected parameter ranges and values are based on established literature.

4.1. Velocity profiles

The influence of key emerging parameters on the nanofluid velocity distribution is systematically illustrated in Figs. 3–7, offering insights into the coupled thermal and entropic behaviour of the unsteady nanofluid flow within a permeable-walled Couette system. Figures 3–5 demonstrate the temporal and spatial evolution of the velocity field, showing that the velocity remains zero at the stationary lower permeable wall due to the no-slip boundary condition, then progressively increases along the channel, attaining its maximum at the upper permeable moving wall. With time, the velocity field transitions from a transient state to a stable steady-state configuration, thereby highlighting the unsteady relaxation mechanisms that govern nanofluid transport. Figure 6 illustrates the influence of nanoparticle volume fraction, where increasing Cu nanoparticle concentration enhances fluid velocity, particularly near the upper moving wall.

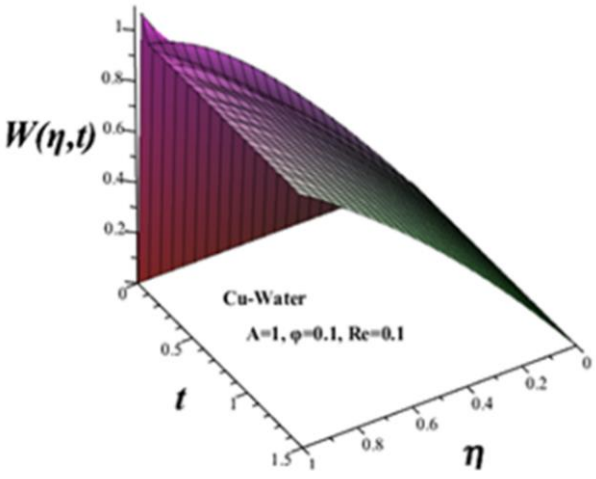

Fig. 3. Variation of the velocity profile with time and space.

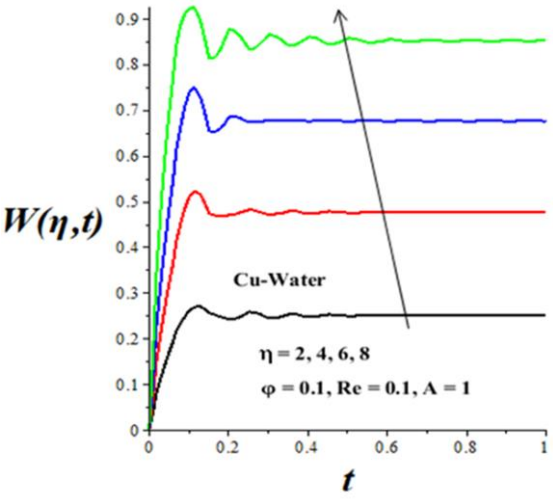

Fig. 4. Impact of η on the velocity profile.

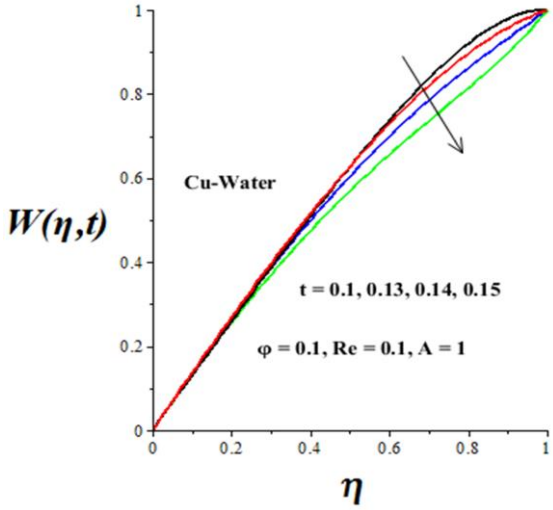

Fig. 5. Impact of t on the velocity profile.

This enhancement stems from the superior thermal conductivity and augmented momentum diffusion imparted by the suspended nanoparticles, which in turn accelerates convective transport and facilitate more effective heat dissipation. Figure 7 emphasises the effect of Reynolds number (Re), showing that higher values intensify the velocity distribution towards the upper moving wall as a result of stronger injection at the lower wall and enhanced suction at the upper wall. This increase in Re not only accelerates the nanofluid flow, but also augments the overall convective heat transfer and entropy generation processes, underscoring the balance between improved thermal performance and irre-

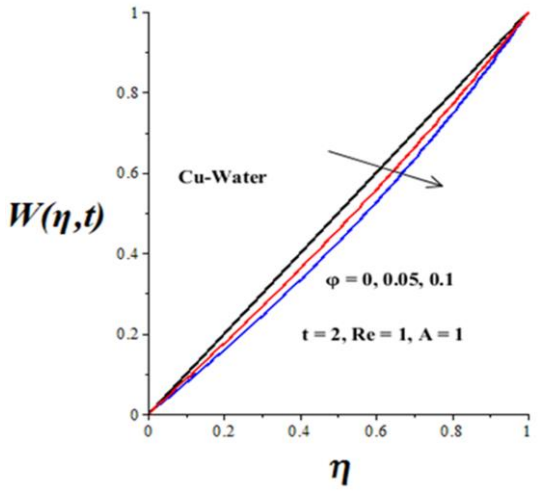

Fig. 6. Impact of φ on the velocity profile.

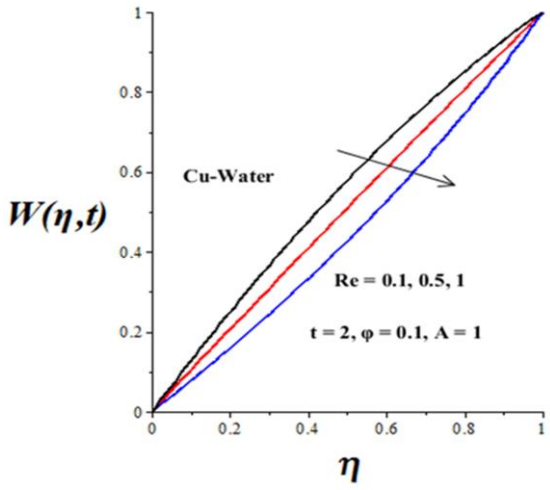

Fig. 7. Impact of Re on the velocity profile.

versibility. From an engineering perspective, these findings carry important implications: the ability to modulate velocity, thermal transport and entropy generation through nanoparticle concentration, wall permeability and flow inertia, offers a pathway for optimising nanofluid-based thermal systems. Applications include advanced cooling strategies in microelectronics and industrial heat exchangers, efficiency enhancement in renewable energy systems such as solar thermal collectors, improved biomedical fluid transport in drug delivery and dialysis devices, and controlled porous filtration in chemical processing. By linking velocity field modifications to thermal and entropic outcomes, this study highlights how tailored parameter tuning in permeable-walled Couette systems can reduce irreversibility, enhance heat management and contributes to the design of energy-efficient, sustainable technologies.

4.2. Temperature profiles

Figures 8–14 present a comprehensive depiction of the thermal and entropic behaviour of unsteady nanofluid flow in a permeable-walled Couette system, highlighting the sensitivity of

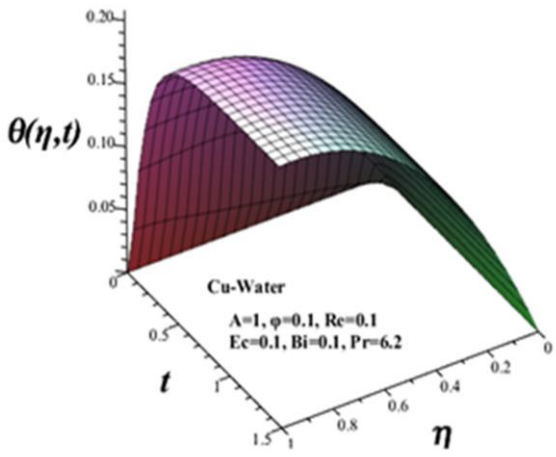

Fig. 8. Variation of the temperature profile with time and space.

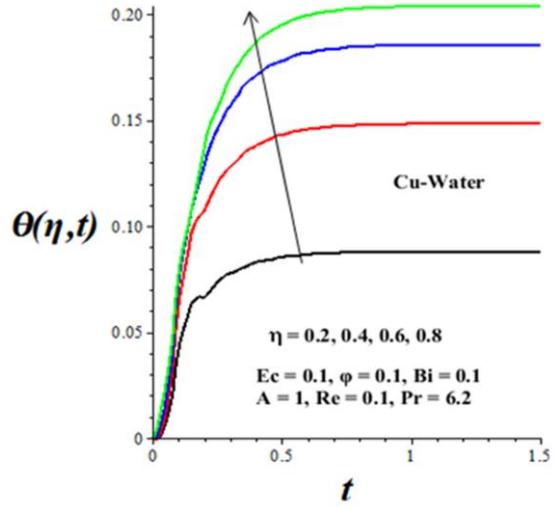

Fig. 9. Impact of η on the temperature profile.

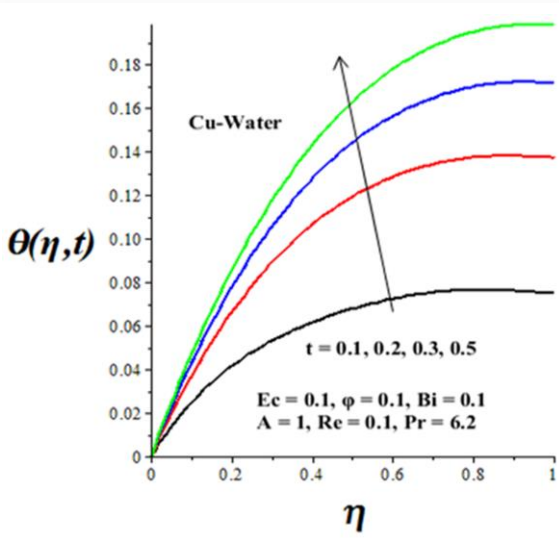

Fig. 10. Impact of t on the temperature profile.

temperature distributions to variations in time, space and key thermophysical parameters. Figures 8–10 demonstrate the transient evolution of the nanofluid temperature profile, where the fluid initially exhibits its lowest temperature at the stationary lower permeable wall due to the imposed boundary conditions. As the fluid migrates upward, the temperature rises progressively under the influence of convective heat transfer at the upper permeable moving wall, eventually stabilising into a steady-state profile over time for fixed parameter values. Figure 11 emphasises the role of Cu nanoparticle volume fraction, showing that higher concentrations increase nanofluid temperature owing to the superior thermal conductivity of metallic nanoparticles, which enhances energy storage and transport across the fluid domain. Similarly, Fig. 12 illustrates the effect of the Eckert number (Ec), where an increase corresponds to greater viscous dissipation and the subsequent conversion of kinetic energy into internal energy, thereby elevating the temperature field.

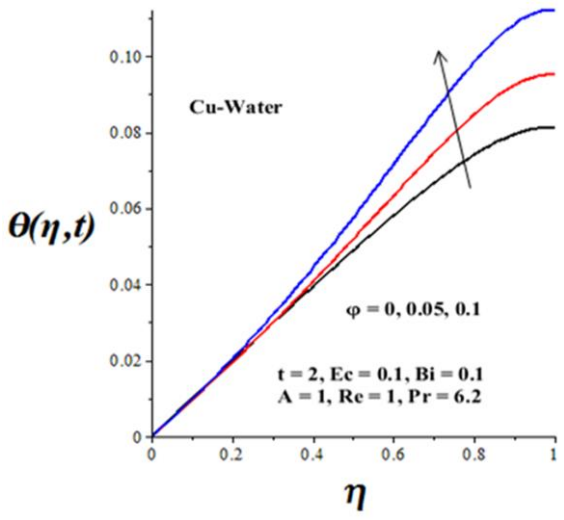

Fig. 11. Impact of φ on the temperature profile.

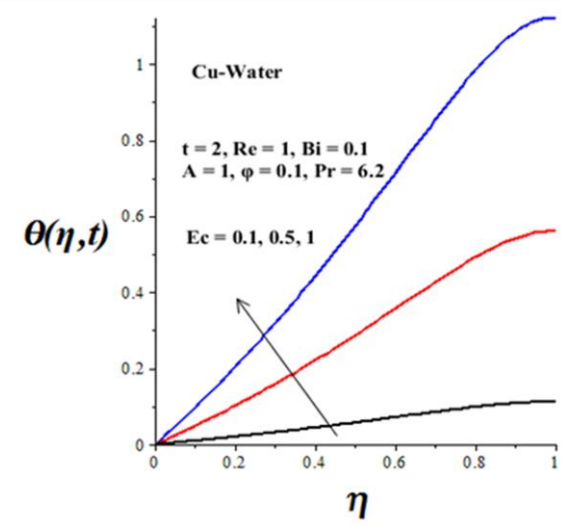

Fig. 12.Impact of Ec on the temperature profile.

In contrast, Figs. 13 and 14 reveal that increasing Reynolds number and Biot number (Bi) leads to notable temperature suppression within the channel. This reduction results from enhanced convective cooling and intensified fluid suction at the upper moving wall, which promotes rapid heat dissipation into

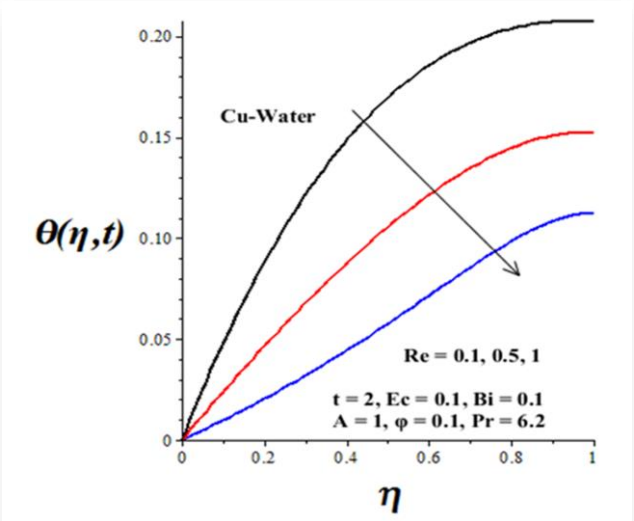

Fig. 13. Impact of Re on the temperature profile.

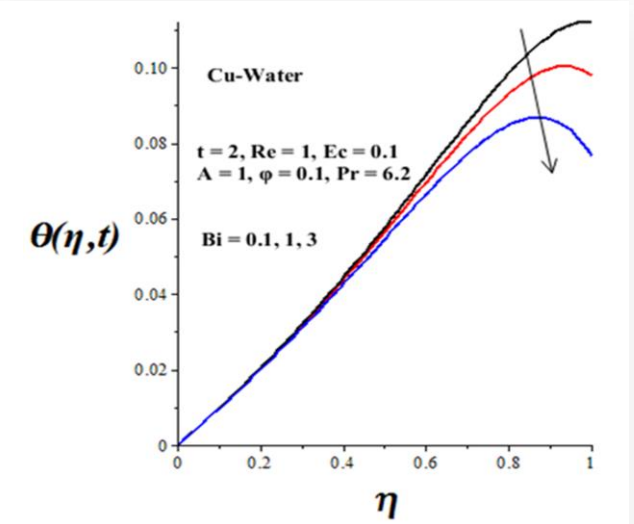

Fig. 14. Impact of Bi on the temperature profile.

the surrounding medium. From an engineering perspective, these findings carry significant implications: the tunability of nanoparticle concentration, viscous dissipation effects and convective boundary conditions provides a pathway for optimising thermal management strategies in high-performance cooling systems, porous filtration processes, microelectronic devices and biomedical applications, where precise regulation of temperature and minimisation of entropy generation are critical. In particular, systems requiring rapid heat removal, such as compact heat exchangers and lab-on-chip devices, benefit from the elevated Re and Bi values, while applications prioritising thermal energy storage or targeted heating, such as photothermal therapy or solar thermal collectors, may exploit

higher nanoparticle concentrations and viscous dissipation effects. Thus, the interplay between thermal and entropic behaviour in permeable-walled Couette systems provides a valuable design framework for developing energy-efficient, sustainable and application-specific nanofluid technologies.

4.3. Skin friction and Nusselt number

Figures 15–17 provide important insights into the coupled thermal and entropic behaviour of unsteady nanofluid flow in a permeable-walled Couette system, with direct implications for engineering applications, where heat transfer efficiency and energy dissipation are critical. The results indicate that an increase in the nanoparticle volume fraction (φ) significantly raises the skin friction at both channel walls, a trend linked to the higher effective viscosity and augmented momentum transport of nanofluids, which intensify wall shear stresses. Specifically, Fig. 15 shows that increasing the Reynolds number enhances skin friction at the upper permeable moving wall due to stronger suction effects, which accelerate near-wall momentum transfer, whereas the opposite trend is observed at the lower permeable stationary wall, where injection weakens shear stress and reduces skin friction. This contrasting behaviour underscores the delicate balance between suction and injection mechanisms in modulating near-wall flow dynamics. Figures 16 and 17 further highlight the influence of thermophysical parameters on the Nusselt number, a measure of convective heat transfer.

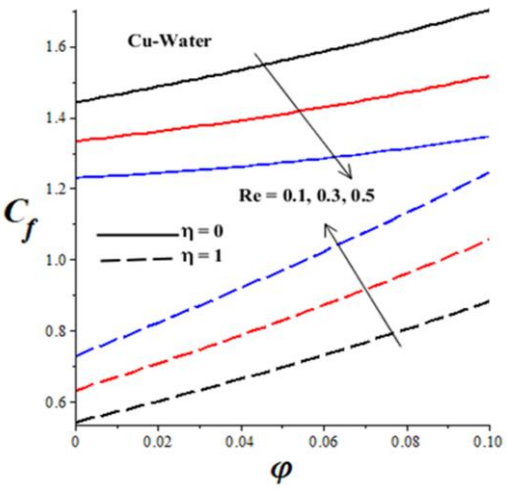

Fig. 15. Impact of Re and φ on skin friction.

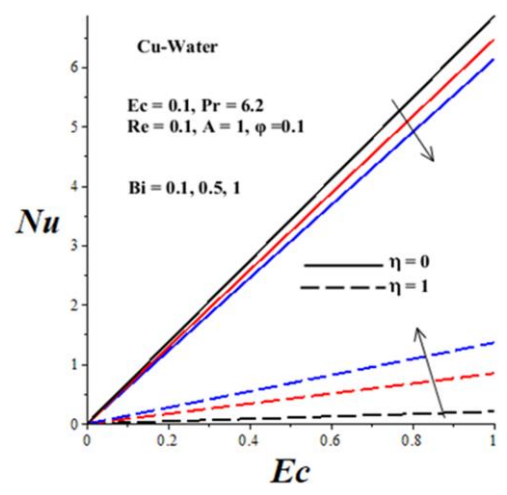

Fig. 16. Impact of Bi and Ec on the Nusselt number.

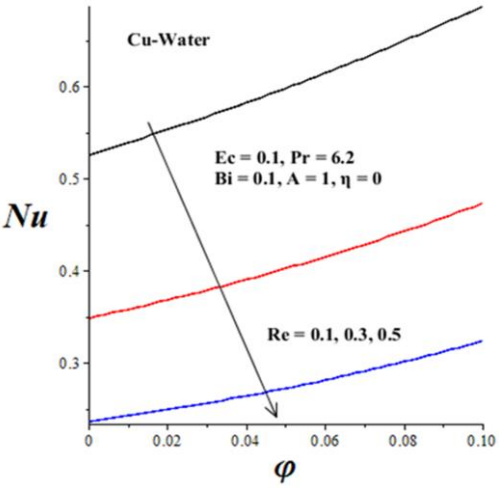

Fig. 17. Impact of Re and φ on the Nusselt number.

The findings reveal that higher nanoparticle volume fraction, Eckert number and Biot number, all contribute to improved convective heat transfer rates. This enhancement is attributed, respectively, to improved thermal conductivity from nanoparticle suspension, increased viscous dissipation and internal heat generation and stronger convective coupling between the fluid and its thermal environment. In contrast, a rise in Re diminishes the Nusselt number, as intensified suction and injection dynamics facilitate stronger convective cooling that dissipates thermal energy more rapidly, thereby lowering the effective heat transfer at the walls. These observations carry important engineering implications: for instance, in microelectronic cooling systems, increasing nanoparticle concentration and optimising viscous dissipation can significantly enhance thermal management, while in porous filtration and biomedical applications, careful regulation of suction and injection is necessary to balance shear stress effects with heat transfer requirements. Similarly, in renewable energy systems, such as solar collectors or geothermal exchangers, tuning Biot and Eckert numbers can improve energy recovery efficiency while minimising entropy generation. Overall, the parametric interplay illustrated in Figs. 15–17 highlights strategies for enhancing heat transfer while mitigating irreversibility, thereby guiding the design of more efficient and sustainable nanofluid-based thermal systems.

4.4. Entropy generation rate

Figures 18–21 present a detailed exploration of the thermal and entropic behaviour of unsteady nanofluid flow in a permeable-walled Couette system, highlighting how emerging flow and thermal parameters influence entropy generation and, by extension, the efficiency of energy transport. A key observation is that

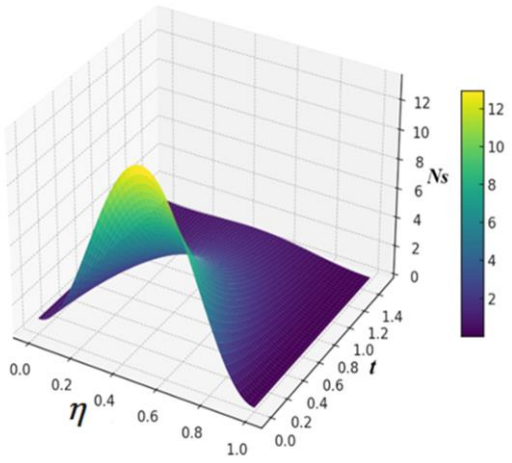

Fig. 18. The entropy generation rate (*Ns*) profile with time and space.

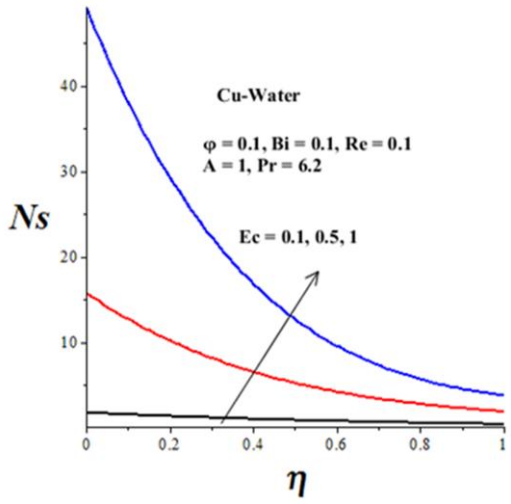

Fig. 20. Impact of Ec on *Ns*.

entropy generation is consistently higher near the lower stationary permeable wall compared to the upper moving wall, a disparity arising from the combined effects of fluid injection at the lower boundary and the modified thermophysical properties of the nanofluid, which accentuate velocity and temperature gradients. Figure 18 provides a three-dimensional surface plot of the entropy generation rate (*Ns*) in the (η,*t*)-space, offering an insightful visualisation of how thermodynamic irreversibility evolves both spatially and temporally. Here, entropy generation is dominated by wall shear stresses and transient start-up effects, with higher values evident at early times and near-wall regions. Over time, as the system progresses toward a quasi-steady state, irreversibility diminishes, indicating stabilisation of both thermal and hydrodynamic fields. This behaviour has significant engineering implications: in microchannel heat exchangers, microelectromechanical systems (MEMS), energy storage devices and biomedical thermal management systems, minimising entropy generation directly translates to improved exergy efficiency, reduced operational losses and more sustainable designs. Figures 19 and 20 show that increasing the copper nanoparticle volume fraction enhances entropy generation due to the dual effect of improved thermal conductivity and elevated viscosity.

While nanoparticles facilitate more efficient heat transfer, the associated viscous resistance increases momentum dissipation, thereby elevating irreversibility, a trade-off engineers must balance when designing nanofluid-based cooling and energy systems.

Similarly, higher Eckert numbers intensify entropy production by converting more mechanical energy into heat through viscous dissipation, underscoring the critical role of flow velocity and shear rates in determining energy efficiency in practical applications, such as turbine blade cooling or biomedical perfusion processes. Figures 21 and 22 further demonstrate the nuanced effects of Biot number and Reynolds number: increasing Bi and Re reduces entropy generation at the lower stationary permeable wall due to stronger convective cooling and fluid injection, which diminishes thermal gradients and lowers irreversibility. Conversely, the upper moving wall exhibits higher entropy production under the same conditions, driven by enhanced

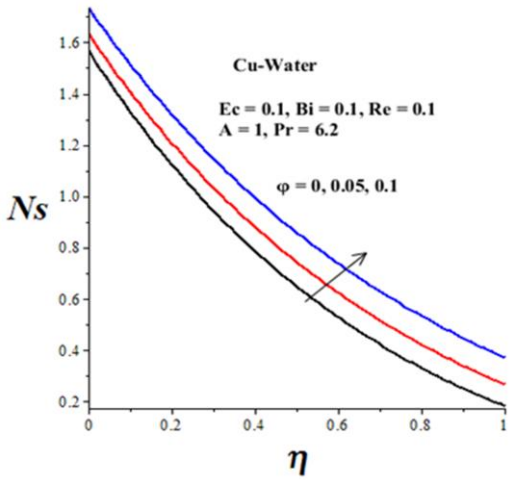

Fig. 19. Impact of φ on *Ns*.

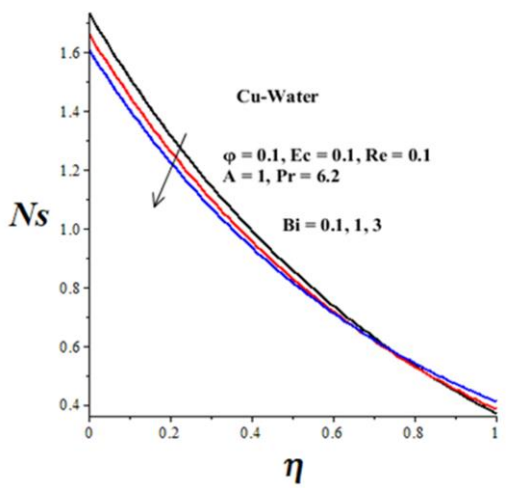

Fig. 21. Impact of Bi on *Ns*.

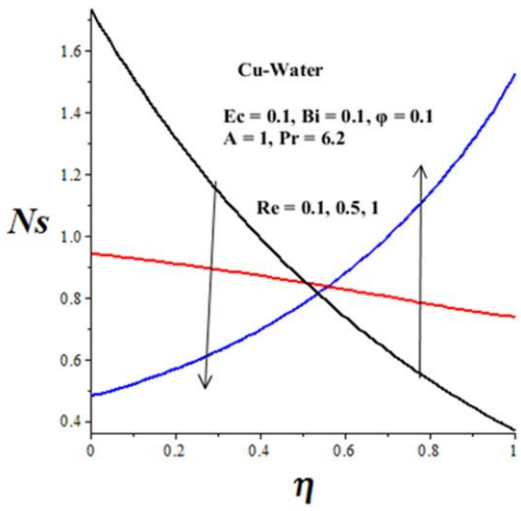

Fig. 22. Impact of Re on *Ns*.

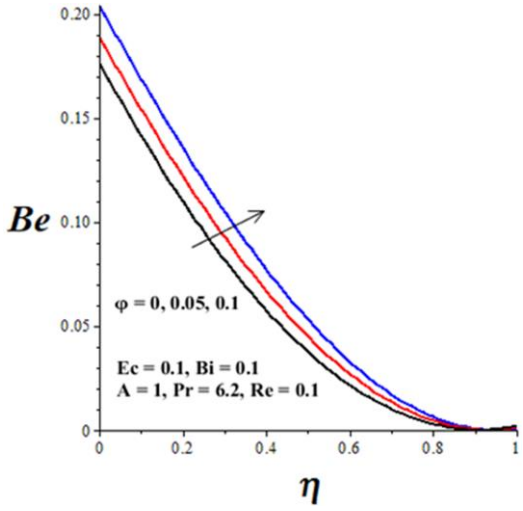

Fig. 23. Impact of φ on Be.

suction effects and amplified convective heat exchange, which strengthen local energy dissipation.

These results emphasise that while parameters, such as nanoparticle concentration and the Eckert number uniformly increase entropy generation, the Biot and Reynolds numbers introduce spatially contrasting behaviours, making entropy distribution highly dependent on wall conditions and flow regulation. From an engineering standpoint, this tunability is advantageous, allowing for tailored optimisation of system performance through strategic manipulation of boundary conditions. For instance, in industrial cooling loops, porous filtration systems or renewable energy collectors, controlling suction/injection rates and wall thermal properties can minimise irreversibility in critical regions, thereby improving efficiency and lowering energy costs. Overall, the thermal and entropic analysis not only deepens the understanding of nanofluid transport in permeable Couette systems, but also provides practical guidance for designing advanced thermal-fluid systems, in which irreversibility hotspots must be identified, controlled and mitigated to achieve sustainable and high-performance energy management.

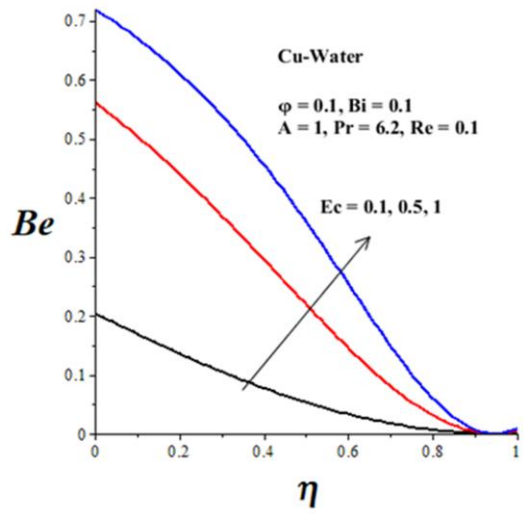

Fig. 24. Impact of Ec on Be.

4.5. Bejan number

Figures 23–26 illustrate the complex influence of key thermophysical and flow parameters on the Bejan number (Be), offering critical insights into the dominant mechanisms of entropy generation within the unsteady nanofluid flow in a permeable-walled Couette system. The Bejan number serves as a vital metric for distinguishing between the relative contributions of heat transfer irreversibility and fluid friction irreversibility to the total entropy generation rate. A higher Bejan number indicates that entropy production is primarily driven by thermal gradients and heat transfer processes, whereas a lower value reflects a predominance of fluid friction and viscous effects. Across the channel, a consistent observation is that the Bejan number is generally higher near the lower stationary permeable wall compared to the upper moving wall, suggesting that thermal irreversibilities are more pronounced in regions influenced by fluid injection and significant temperature gradients. The analysis shows that increasing the Cu

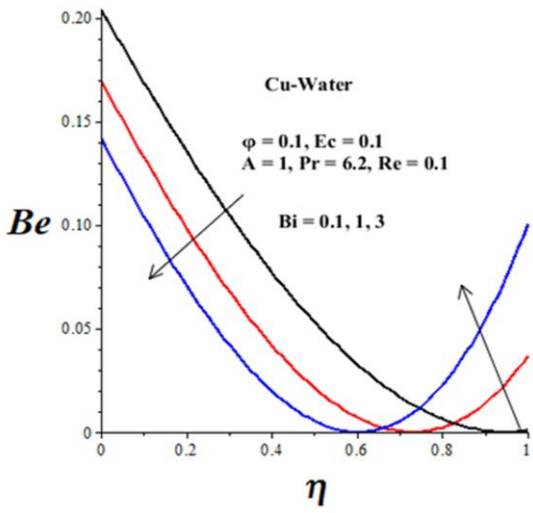

Fig. 25. Impact of Bi on Be.

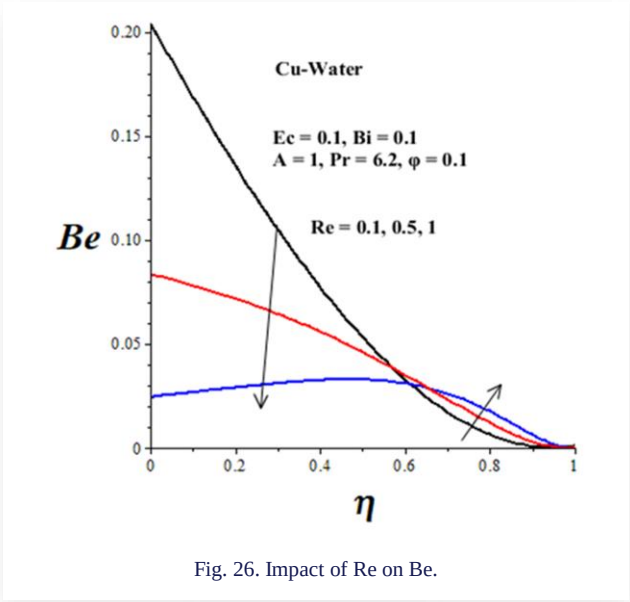

Fig. 26. Impact of Re on Be.

nanoparticle volume fraction and the Eckert number leads to a marked elevation in the Bejan number. Higher nanoparticle concentrations enhance the effective thermal conductivity of the nanofluid, facilitating more efficient heat transport and consequently increasing the dominance of heat transfer-related entropy generation. Similarly, larger Eckert numbers, representing the conversion of kinetic energy into internal energy through viscous dissipation, further amplify thermal irreversibility, elevating the Bejan number throughout the channel.

From an engineering perspective, these findings indicate that carefully tuning nanoparticle concentration and controlling flow velocities to modulate viscous heating can enhance thermal management efficiency in systems, such as microchannel heat exchangers, electronic cooling devices and solar thermal collectors, where minimising entropy generation is critical for performance optimisation. In contrast, the Biot number and the injection/suction Reynolds number exhibit spatially dependent effects on the Bejan number. At the lower stationary wall, increasing Bi and Re results in a decrease in the Bejan number, signalling that fluid friction irreversibility becomes more dominant. This reduction arises from enhanced convective cooling and intensified fluid injection, which reduce local temperature gradients and shift the primary source of entropy generation towards shear-induced losses.

Conversely, at the upper moving wall, increasing the Biot and Reynolds numbers elevates the Bejan number, reflecting an intensified role of thermal irreversibility due to stronger fluid suction and augmented convective heat transfer at this boundary. This spatial variation in entropy generation mechanisms underscores the importance of localised flow and thermal control strategies for optimising system performance, particularly in applications involving porous surfaces, microfluidic devices, or biomedical cooling systems, where precise thermal regulation is critical. Overall, these results highlight that while parameters, such as nanoparticle volume fraction and Eckert number, consistently enhance heat transfer irreversibility across the channel, parameters like Bi and Re exert location-specific effects, producing complex distributions of entropy generation. Understanding these trends is essential for engineering design strategies aimed at reducing energy losses, improving heat transfer efficiency, and developing more sustainable and high-performance nanofluid-based flow systems.

6. Conclusions

This study presents a detailed numerical investigation of unsteady Cu-water nanofluid flow in a permeable-walled Couette system with convective heat transfer, employing a semi-discretisation finite-difference method coupled with a Runge-Kutta-Fehlberg integration scheme. Entropy generation was analysed through velocity and temperature gradients, providing insights into the interplay between thermal and viscous irreversibilities. The influence of key thermophysical and flow parameters on velocity, temperature, skin friction, Nusselt number, entropy generation rate and Bejan number was systematically examined, revealing several notable trends with direct relevance to engineering applications. The key conclusions from this study are as follows:

- The nanofluid velocity and temperature fields evolve dynamically over time, ultimately stabilising into steady-state profiles within the channel. This behaviour is critical for engineering systems, where predictable thermal and flow performance is essential, such as in microchannel heat exchangers and cooling devices for electronics.
- Increasing the nanoparticle volume fraction and the injection/suction Reynolds number enhances the velocity distribution toward the upper moving permeable wall. This indicates that manipulating nanoparticle concentration and flow intensity can effectively control fluid transport and shear rates, which is beneficial for applications requiring targeted convective enhancement, such as industrial cooling channels and biomedical microfluidic systems.
- The nanofluid temperature rises with higher solid volume fraction and Eckert number, reflecting improved thermal conductivity due to nanoparticles and increased viscous dissipation, while it decreases with higher Reynolds and Biot numbers, highlighting the influence of flow-induced cooling and convective heat transfer. Understanding these trends is vital for thermal management in high-heat-flux devices, solar collectors and other energy systems, where precise temperature control is required.
- Higher nanoparticle volume fraction leads to increased skin friction, Nusselt number, entropy generation rate and Bejan number, emphasising that enhanced heat transfer is accompanied by greater thermal irreversibility. Similarly, higher Eckert numbers amplify heat transfer and entropy production, underlining the trade-offs between viscous heating and thermal efficiency. These insights are important for designing systems where maximising heat transfer must be balanced against minimising energy losses, such as in advanced cooling technologies and energy-efficient nanofluid-based heat exchangers.

- The effects of the Reynolds and Biot numbers are spatially dependent: increasing the Reynolds number reduces skin friction, the Nusselt number, the entropy generation and the Bejan number at the lower stationary wall, but increases them at the upper moving wall. Likewise, a higher Biot number decreases these quantities at the lower wall while enhancing them at the upper wall. These variations underscore the critical role of boundary-layer control, fluid injection/suction and convective conditions in optimising both thermal performance and energy efficiency in engineering applications, including porous channels, microfluidic devices and industrial thermal management systems.

Finally, understanding the spatial and parametric dependencies of entropy generation and heat transfer provides a framework for optimising nanofluid-based systems, enabling engineers to maximise thermal performance while minimising irreversibility, ultimately contributing to more sustainable and energy-efficient technologies. For the future, the model may be extended to include the combined effects of other physical factors, such as magnetic field, thermal radiation, buoyancy forces, Joule heating, thermophoresis and Brownian motion.

References

[1] Bejan, A. (1995). *Entropy generation minimization*: *The method of thermodynamic optimization of finite-size systems and finite-time processes*. CRC Press, Boca Raton.

[2] Das, S.K., Choi, S.U.S, & Patel, H.E. (2006). Heat transfer in nanofluids − A review. *Heat Transfer Engineering*, 27(10), 3−19. doi: 10.1080/01457630600904593

[3] Choi, S.U.S. (1995). Enhancing thermal conductivity of fluids with nanoparticles. In *Developments and applications of non-Newtonian flows*. ASME FED, 231/MD 66 (pp. 99–105), New York.

[4] Narmatha, M., & Kavitha, R. (2024). Analysis of unsteady heat and mass transfer in rotating MHD convection flow over a porous vertical plate. *Archives of Thermodynamics*, 45(4), 179−187. doi: 10.24425/ather.2024.152007

[5] Batchelor, G.K. (2000). *An introduction to fluid dynamics*. Cambridge University Press.

[6] Abu-Nada, E. & Chamkha, A.J. (2010). Mixed convection flow in a lid-driven inclined square enclosure filled with a nanofluid. *European Journal of Mechanics B/Fluids*, 29(6), 472–482. doi: 10.1016/j.euromechflu.2010.06.008

[7] Ali, K., Rajashekar Reddy, Y., & Balla, C.S. (2021). Numerical solution of transient Fe_3O_4-EG nanofluid past the Couette channel associated with radiation. *International Journal of Ambient Energy*, 43(1), 5673–5686. doi: 10.1080/01430750.2021.1970623

[8] Nield, D.A., & Bejan, A. (2006). *Convection in porous media*. Springer. doi: 10.1007/978-3-319-49562-0

[9] Kasaeian, A., Daneshazarian, R., Mahian, O., Kolsi, L., Chamkha, A.J., Wongwises, S., & Pop, I. (2017). Nanofluid flow and heat transfer in porous media: A review of the latest developments. *International Journal of Heat and Mass Transfer*, 107, 778−791. doi: 10.1016/j.ijheatmasstransfer.2016.11.074

[10] Kakac, S. & Pramuanjaroenkij, A. (2009). Review of convective heat transfer with nanofluids. *International Journal of Heat and Mass Transfer*, 52(13-14), 3187–3196. doi: 10.1016/j.ijheatmasstransfer.2009.02.006

[11] Shanthi, R., Anandan, S.S., & Ramalingam, V. (2012). Heat transfer enhancement using nanofluids: An overview. *Thermal Science*, 16(2), 423–444. doi: 10.2298/TSCI110201003S

[12] Malik, Z.U., Mallawi, F.O., & Haq, R.U. (2021). Thermal energy performance of nanofluid flow and heat transfer vertical channel with permeable surface. *Case Studies in Thermal Engineering*, 28, 101447. doi: 10.1016/j.csite.2021.101447

[13] Mkwizu, M.H., & Makinde, O.D. (2015). Entropy generation in variable viscosity channel flow of nanofluids with convective cooling. *Comptes Rendus Mecanique*, 343(1), 38−56. doi: 10.1016/j.crme.2014.09.002

[14] Ndelwa, E.J., Mkwizu, M.H., Matofali, A.X., & Ali, A.O. (2025). Thermodynamic analysis of entropy generation in MHD hybrid nanofluid channel flow under Navier slip conditions. *International Journal of Ambient Energy*, 46(1), 2559148. doi: 10.1080/01430750.2025.2559148

[15] Oztop, H.F., & Abu-Nada, E. (2008). Numerical study of natural convection in partially heated rectangular enclosures filled with nanofluids. *International Journal of Heat and Fluid Flow*, 29(5), 1326–1336. doi: 10.1016/j.ijheatfluidflow.2008.04.009

[16] Siddabasappa, Siddheshwar, P.G. & Makinde, O.D. (2021). A study of entropy generation and heat transfer in a magnetohydrodynamics flow of a couple-stress fluid through a thermal non-equilibrium vertical porous channel. *Heat Transfer*, 50(6), 6377–6400. doi: 10.1002/htj.22176

[17] Rikitu, E.H., & Makinde, O.D. (2024). Entropy generation and heat transfer analysis of Eyring-Powell nanofluid flow through inclined microchannel subjected to magnetohydrodynamics and heat generation. *International Journal of Thermofluids*, 22, 100640. doi: 10.1016/j.ijft.2024.100640

[18] Ali, R., Iqbal, A., Abbass, T., Arshad, T., & Shahzad, A. (2024). Unsteady flow of silica nanofluid over a stretching cylinder with effects of different shapes of nanoparticles and Joule heating. *Archives of Thermodynamics*, 45(3), 115−126. doi: 10.24425/ather.2024.151222

[19] Gao, X.W., Zhu, Y.-M., & Pan, T. (2023). Finite line method for solving high-order partial differential equations in science and engineering. *Partial Differential Equations in Applied Mathematics*, 7, 100477. doi: 10.1016/j.padiff.2022.100477

[20] Gorai, V.K., Kumar, M., Singh, R., & Sahu, M.K. (2025). Theoretical investigation for optimal thermal and thermodynamic performance of flat-plate solar collector with nanofluids. *Archives of Thermodynamics*, 46(1), 155–167. doi: 10.24425/ ather.2025.154189

[21] Makinde, O.D., & Eegunjobi, A.S. (2013). Effects of convective heating on entropy generation rate in a channel with permeable walls. *Entropy*, 15(1), 220−233. doi: 10.3390/e15010220